CHAPTER – 6

ANALYSIS OF VIBRATIONAL SPECTRA OF 4-AMINO-*N*-(4-METHYL-2-PYRIMIDINYL)BENZENESULFONAMIDE (SULFAMERAZINE) BASED ON DENSITY FUNCTIONAL THEORY CALCULATIONS

Sulfonamides were the first synthetic antibacterial agents which inhibit bacterial growth by interfering with bacterial folic acid synthesis. Sulfonamide derivatives are known for their antibacterial, antidiabetic, carbonic anhydrase inhibiting and antithyroid properties [124]. The organic compound 4-Amino-*N*-(4-methyl-2-pyrimidinyl)benzenesulfonamide, commonly known as sulfamerazine, is an antibacterial drug belonged to sulfonamide group of compounds. Sulfamerazine with other sulfanilamide derivatives is effective in the treatment of bacterial infections in children [125]. In the reported structure of sulfamerazine [126], the hydrogen-bonded network is formed by intermolecular N−H···N and N−H···O hydrogen bonds.

Copper (II) and Nickel (II) complexes of sulfonamide ligands including sulfamerazine is found to have antiseptic activity of the metal associated with the antibiotic activity of the ligand [127]. A density functional theory investigation of sulfamerazine and sulfathiazole reveals the important role of nitrogen nuclei in formation of H-bonding interactions [128]. In the crystallization studies of sulfamerazine, it is shown that the polymorphs can be controlled by optimizing the use of ultrasonic irradiation [129]. The solvates and a monohydrate of N^4-acetylsulfamerazine have been studied using nuclear magnetic resonance spectroscopy and thermochemical analysis [130]. The cocrystallization behaviors of sulfamerazine and sulfamethazine with p-aminobenzoic acid are studied [131]. The

aim of this work is to predict the vibrational spectra of sulfamerazine with the aid of density functional theory methods using B3LYP/6-311G(d, p) basis set. A complete vibrational assignment of the title compound has been done by utilizing normal coordinate analysis (NCA) followed by scaled quantum mechanical (SQM) force field calculations.

6.1 Experimental details

The sulfamerazine compound of 98% purity was purchased from Sigma-Aldrich and the solid sample was dissolved in dimethylformamide. The solution is left for crystallization by slow evaporation of the solvent at room temperature. Colorless block crystals obtained were subjected to record FT-IR and FT-Raman spectra in the region 4000 − 400 cm^{-1} using Jasco FT/IR-6300 and in the region 3500 − 50 cm^{-1} using FT RAMAN Bruker RFS 100/S Spectrometer respectively. The resolution of both the spectra is 4 cm^{-1}. An air-cooled Nd: YAG laser at 1064 nm wavelength with an output of 150 mW power was used as an exciting source and the standard Germanium was used as the detector. The UV-visible spectrum of sulfamerazine was recorded in the dimethylformamide solvent using a Cary 5E UV-VIS-NIR spectrophotometer.

6.2 Optimized geometries

The sulfamerazine molecule consists of a pyrimidine ring and a phenyl ring linked by a SO_2NH group. The optimized molecular structure of sulfamerazine is shown in Fig. 6.1 and the computed geometries given in Tables 6.1 and 6.2 are compared with the XRD data [126]. The C−C bond lengths of pyrimidine ring are 1.391 and 1.396 Å. The C−N bond lengths vary from 1.331 – 1.341 Å, the distortion

in the bond lengths is due to the substitution of electron donating methyl group to the pyrimidine ring. The difference between bond lengths S_{15}–O_{16} and S_{15}–O_{16} is 0.011 Å experimentally while that of calculated value is 0.006 Å. This is due to the involvement of one S=O in N–H···O intermolecular interaction in the crystalline state. There is no significant effect on the angles due to the methyl group substitution in the heterocyclic ring when compared to the pyrimidine geometry [132].

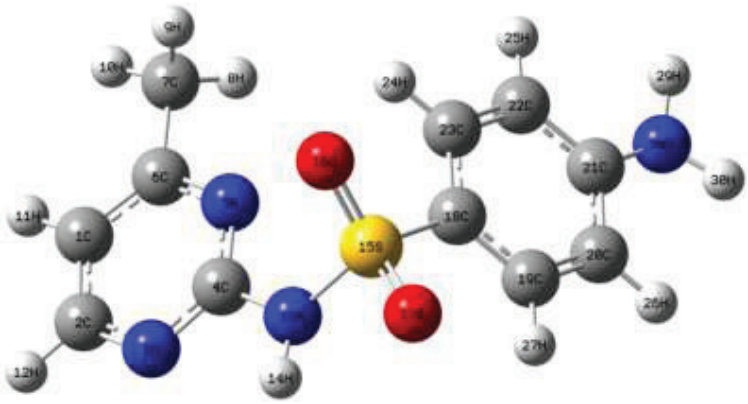

Fig. 6.1 Optimized molecular structure and atomic numbering of sulfamerazine.

The phenyl ring loses its symmetry due to the substituents. The bond lengths of phenyl ring varies from 1.378 – 1.407 Å due to the conjugation of electron donating amine group in the ring system. The bond angle C_{20}–C_{21}–C_{22} (118.7°) is reduced when compared with the typical hexagonal angle of 120° due to the substitution of the electron donating amine group to the phenyl ring.

Table 6.1 Selected bond lengths and bond angles of sulfamerazine by B3LYP/ 6-311G (d, p) in comparison with the XRD data.

Bond length	Calc. (Å)	Expt. [126] (Å)	Bond angle	Calc. (°)	Expt. [126] (°)
C_1–C_2	1.391	1.373	C_2–C_1–C_6	116.94	117.72
C_1–C_6	1.396	1.374	C_2–C_1–H_{11}	121.39	121.11
C_1–H_{11}	1.082	0.950	C_6–C_1–H_{11}	121.67	121.17
C_2–N_3	1.331	1.336	C_1–C_2–N_3	122.88	122.90
C_2–H_{12}	1.087	0.951	C_1–C_2–H_{12}	121.01	118.56
N_3–C_4	1.341	1.337	C_3–C_2–H_{12}	116.10	118.54
C_4–N_5	1.332	1.327	C_2–N_3–C_4	115.17	114.59
C_4–N_{13}	1.388	1.389	N_3–C_4–N_5	127.28	127.53
N_5–C_6	1.339	1.345	N_3–C_4–N_{13}	114.54	113.96
C_6–C_7	1.503	1.500	N_5–C_4–N_{13}	118.16	118.51
C_7–H_8	1.093	0.980	C_4–N_5–C_6	116.70	116.22
C_7–H_9	1.093	0.980	C_1–C_6–N_5	121.01	121.02
C_7–H_{10}	1.091	0.981	C_1–C_6–C_7	122.43	123.03
N_{13}–H_{14}	1.013	0.880	N_5–C_6–C_7	116.55	115.95
N_{13}–S_{15}	1.709	1.653	C_6–C_7–H_8	109.89	109.46
S_{15}–O_{16}	1.454	1.429	C_6–C_7–H_9	109.79	109.51
S_{15}–O_{17}	1.460	1.440	C_6–C_7–H_{10}	111.84	109.49
S_{15}–C_{18}	1.777	1.734	H_8–C_7–H_9	107.23	109.47
C_{18}–C_{19}	1.396	1.389	H_8–C_7–H_{10}	109.03	109.46
C_{18}–C_{23}	1.394	1.399	H_9–C_7–H_{10}	108.94	109.44
C_{19}–C_{20}	1.385	1.381	C_4–N_{13}–H_{14}	115.36	116.85
C_{19}–H_{27}	1.083	0.949	C_4–N_{13}–S_{15}	126.87	126.22
C_{20}–C_{21}	1.408	1.407	H_{14}–N_{13}–S_{15}	112.38	116.93
C_{20}–H_{26}	1.085	0.950	N_{13}–S_{15}–O_{16}	109.95	109.05
C_{21}–C_{22}	1.407	1.404	N_{13}–S_{15}–O_{17}	101.52	102.31
C_{21}–N_{28}	1.382	1.364	N_{13}–S_{15}–C_{18}	104.83	106.59
C_{22}–C_{23}	1.385	1.378	O_{16}–S_{15}–O_{17}	121.53	119.28
C_{22}–H_{25}	1.085	0.950	O_{16}–S_{15}–C_{18}	108.81	109.54
C_{23}–H_{24}	1.081	0.950	O_{17}–S_{15}–C_{18}	108.86	109.21
N_{28}–H_{29}	1.008	0.881	S_{15}–C_{18}–C_{19}	119.33	119.58
N_{28}–H_{30}	1.008	0.880	S_{15}–C_{18}–C_{23}	120.00	120.38
-	-	-	C_{19}–C_{18}–C_{23}	120.65	120.04

Bond length	Calc. (Å)	Expt. [126] (Å)	Bond angle	Calc. (°)	Expt. [126] (°)
-	-	-	$C_{18}–C_{19}–C_{20}$	119.67	120.37
-	-	-	$C_{19}–C_{20}–C_{21}$	120.65	120.23
-	-	-	$C_{20}–C_{21}–N_{28}$	120.60	120.83
-	-	-	$C_{22}–C_{21}–N_{28}$	120.66	120.46
-	-	-	$C_{21}–C_{22}–C_{23}$	120.76	120.92
-	-	-	$C_{18}–C_{23}–C_{22}$	119.57	119.69
-	-	-	$C_{21}–N_{28}–H_{29}$	116.88	120.01
-	-	-	$C_{21}–N_{28}–H_{30}$	116.90	120.02
-	-	-	$H_{29}–N_{28}–H_{30}$	113.61	119.97

Table 6.2 Selected dihedral angles of sulfamerazine by B3LYP/ 6-311G (d, p) in comparison with the XRD data.

Dihedral angle	Calc. (°)	Expt. [126] (°)
$C_6–C_1–C_2–N_3$	0.58	0.33
$C_6–C_1–C_2–H_{12}$	-179.74	-179.60
$H_{11}–C_1–C_2–N_3$	-179.45	-179.65
$H_{11}–C_1–C_2–H_{12}$	0.23	0.43
$C_2–C_1–C_6–N_5$	0.15	-0.92
$C_2–C_1–C_6–C_7$	180	178.19
$C_1–C_2–N_3–C_4$	-0.54	0.89
$H_{12}–C_2–N_3–C_4$	179.77	-179.18
$C_2–N_3–C_4–N_5$	-0.25	-1.75
$C_2–N_3–C_4–N_{13}$	-178.34	178.47
$N_3–C_4–N_5–C_6$	0.94	1.21
$N_{13}–C_4–N_5–C_6$	178.96	-179.02
$N_3–C_4–N_{13}–H_{14}$	-6.36	-7.39
$N_3–C_4–N_{13}–S_{15}$	-158.25	172.59
$N_5–C_4–N_{13}–H_{14}$	175.36	172.81
$N_5–C_4–N_{13}–S_{15}$	23.47	-7.21
$C_4–N_5–C_6–C_1$	-0.83	0.23
$C_4–N_5–C_6–C_7$	179.31	-178.94
$C_1–C_6–C_7–H_8$	-122.40	-122.42
$C_1–C_6–C_7–H_9$	119.89	117.57
$C_1–C_6–C_7–H_{10}$	-1.16	-2.43

Dihedral angle	Calc. (°)	Expt. [126] (°)
C_5–C_6–C_7–H_8	57.46	56.73
C_5–C_6–C_7–H_9	-60.25	-63.28
C_5–C_6–C_7–H_{10}	178.70	176.72
C_4–N_{13}–S_{15}–O_{16}	37.60	53.48
C_4–N_{13}–S_{15}–O_{17}	167.53	-179.29
C_4–N_{13}–S_{15}–C_{18}	-79.20	-64.69
H_{14}–N_{13}–S_{15}–O_{16}	-114.98	-126.54
H_{14}–N_{13}–S_{15}–O_{17}	14.94	0.69
H_{14}–N_{13}–S_{15}–C_{18}	128.22	115.29
N_{13}–S_{15}–C_{18}–C_{19}	-83.35	-84.65
N_{13}–S_{15}–C_{18}–C_{23}	98.38	94.25
O_{16}–S_{15}–C_{18}–C_{19}	159.06	157.50
O_{16}–S_{15}–C_{18}–C_{23}	-19.20	-23.60
O_{17}–S_{15}–C_{18}–C_{19}	24.63	25.19
O_{17}–S_{15}–C_{18}–C_{23}	-153.64	-155.91
S_{15}–C_{18}–C_{19}–C_{20}	-178.43	177.38
C_{23}–C_{18}–C_{19}–C_{20}	-0.18	-1.53
S_{15}–C_{18}–C_{23}–C_{22}	178.28	-177.32
C_{19}–C_{18}–C_{23}–C_{22}	0.04	1.57
C_{18}–C_{19}–C_{20}–H_{26}	179.77	179.59
H_{27}–C_{19}–C_{20}–C_{21}	-178.47	179.62
H_{27}–C_{19}–C_{20}–H_{26}	1.15	-0.40
C_{19}–C_{20}–C_{21}–C_{22}	0.01	2.22
C_{19}–C_{20}–C_{21}–N_{28}	-177.73	-178.97
H_{26}–C_{20}–C_{21}–C_{22}	-179.61	-177.76
H_{26}–C_{20}–C_{21}–N_{28}	2.65	1.05
C_{20}–C_{21}–C_{22}–C_{23}	-0.15	-2.18
C_{20}–C_{21}–C_{22}–H_{25}	179.78	177.75
N_{28}–C_{21}–C_{22}–C_{23}	177.59	179.00
N_{28}–C_{21}–C_{22}–H_{25}	-2.49	-1.07
C_{20}–C_{21}–N_{28}–H_{29}	-160.82	-178.71
C_{20}–C_{21}–N_{28}–H_{30}	-21.30	1.24
C_{22}–C_{21}–N_{28}–H_{29}	21.49	0.08
C_{22}–C_{21}–N_{28}–H_{30}	161.00	-179.98

6.3 Natural bond orbital analysis

The second order perturbative estimates of donor-acceptor interactions of sulfamerazine are presented in Table 6.3. The delocalization of electrons in the pyrimidine ring is shown by the orbital overlap between the $\pi(C_1-C_2)$ and $\pi^*(N_3-C_4)$, $\pi^*(N_5-C_6)$ resulting in the stabilization energy of 11.99 and 35.97 kcalmol^{-1} respectively. Another energetic interaction is of $\pi(N_3-C_4)$ and $\pi(N_5-C_6)$ with $\pi^*(C_1-C_2)$ and $\pi^*(N_3-C_4)$ resulting in energies 32.81 and 38.61 kcalmol^{-1} respectively. The charge transfer from the electron donating methyl group to the pyrimidine ring is revealed by the hyperconjugative interaction of the methyl orbitals $\sigma(C_7-H_8)$, $\sigma(C_7-H_9)$ and $\sigma(C_7-H_{10})$ with the antibonding orbitals (C_1-C_6) and (N_5-C_6) of the ring. The stabilization energy of 31.85 kcalmol^{-1} shows that the lone pair electron gets donated from the N_{28} atom of the electron donating amine group into the phenyl system [$n_1(N_{28})\rightarrow\pi^*(C_{21}-C_{22})$].

Table 6.3 Second order perturbation theory analysis of Fock matrix in NBO basis.

Donor NBO (i)	Acceptor NBO (j)	E(2)[a] kcal/mol	E(j)-E(i)[b] a.u.	F(i, j)[c] a.u.
$\pi(C_1-C_2)$	$\pi^*(N_3-C_4)$	11.99	0.26	0.051
	$\pi^*(N_5-C_6)$	35.97	0.27	0.089
$\pi(N_3-C_4)$	$\pi^*(C_1-C_2)$	32.81	0.33	0.093
	$\pi^*(N_5-C_6)$	8.62	0.31	0.047
$\pi(N_5-C_6)$	$\pi^*(C_1-C_2)$	9.52	0.32	0.05
	$\pi^*(N_3-C_4)$	38.61	0.3	0.1
$\sigma(C_7-H_8)$	$\sigma^*(C_1-C_6)$	2.24	1.07	0.044
$\sigma(C_7-H_8)$	$\pi^*(N_5-C_6)$	3.93	0.51	0.044
$\sigma(C_7-H_9)$	$\sigma^*(C_1-C_6)$	2.08	1.07	0.042
$\sigma(C_7-H_9)$	$\pi^*(N_5-C_6)$	4.3	0.51	0.046
$\sigma(C_7-H_{10})$	$\sigma^*(N_5-C_6)$	4.5	1.04	0.061

$\pi(C_{18}–C_{23})$	$\sigma^*(N_{13}–S_{15})$	5.75	0.38	0.042
	$\pi^*(C_{19}–C_{20})$	25.22	0.29	0.077
$\pi(C_{18}–C_{23})$	$\pi^*(C_{21}–C_{22})$	13.68	0.29	0.057
$\sigma(C_{19}–C_{20})$	$\sigma^*(S_{15}–C_{18})$	4.19	0.88	0.056
	$\sigma^*(C_{18}–C_{19})$	4.15	1.27	0.065
$\pi(C_{19}–C_{20})$	$\pi^*(C_{18}–C_{23})$	14.55	0.28	0.059
	$\pi^*(C_{21}–C_{22})$	23.45	0.28	0.075
$\pi(C_{21}–C_{22})$	$\pi^*(C_{18}–C_{23})$	30.02	0.28	0.082
	$\pi^*(C_{19}–C_{20})$	14.71	0.29	0.059
$\sigma(C_{22}–C_{23})$	$\sigma^*(S_{15}–C_{18})$	4.27	0.88	0.057
$\sigma(N_{28}–H_{29})$	$\sigma^*(C_{20}–C_{21})$	4.13	1.21	0.063
$\sigma(N_{28}–H_{30})$	$\sigma^*(C_{21}–C_{22})$	4.13	1.21	0.063
$n_1(N_3)$	$\sigma^*(C_1–C_2)$	8.73	0.91	0.081
	$\sigma^*(C_4–N_5)$	11.85	0.88	0.092
$n_1(N_5)$	$\sigma^*(C_1–C_6)$	9.43	0.91	0.084
	$\sigma^*(N_3–C_4)$	12.09	0.86	0.092
$n_1(N_{13})$	$\pi^*(N_3–C_4)$	37.02	0.29	0.098
	$\sigma^*(S_{15}–O_{16})$	6.03	0.6	0.055
$n_3(O_{16})$	$\sigma^*(N_{13}–S_{15})$	20.46	0.39	0.081
	$\sigma^*(S_{15}–O_{17})$	15.96	0.58	0.088
$n_2(O_{17})$	$\sigma^*(N_{13}–S_{15})$	11.96	0.4	0.063
	$\sigma^*(S_{15}–C_{18})$	15.05	0.46	0.075
$n_3(O_{17})$	$\sigma^*(N_{13}–S_{15})$	11.71	0.4	0.062
	$\sigma^*(S_{15}–O_{16})$	19.19	0.59	0.096
$n_1(N_{28})$	$\pi^*(C_{21}–C_{22})$	31.85	0.32	0.095
$\pi^*(N_3–C_4)$	$\pi^*(C_1–C_2)$	121.67	0.02	0.077
	$\pi^*(N_5–C_6)$	290.61	0.01	0.08
$\pi^*(N_5–C_6)$	$\pi^*(C_1–C_2)$	269.14	0.01	0.083
$\pi^*(C_{18}–C_{23})$	$\sigma^*(N_{13}–S_{15})$	7.38	0.09	0.04

[a]E(2) is the energy of hyperconjugative interactions.
[b]Energy difference between donor and acceptor i and j NBO orbitals.
[c]F(i,j) is the Fock matrix element between i and j NBO orbitals.

6.4 Electron localization function (ELF) analysis

Table 6.4 shows the different types of electronic basins, the basin populations (N), standard deviation (σ^2), and relative fluctuation (λ) in the compound sulfamerazine. Fig. 6.2 displays the localization domains of sulfamerazine bounded by $\eta(r) = 0.8$ isosurface. Relative fluctuation is a good measure of the delocalization [133], which is usually of the order of 0.1 for core basins, 0.3 for basin of the protonated disynaptic attractor, 0.4 for basins related to single and double C–C bonds and 0.5 for delocalized bonds. The analysis of electron localization function of sulfamerazine shows that there is 11 carbon, 4 nitrogen, 1 sulfur and 2 oxygen core basins. The relative fluctuation of all the core basins is in the order of 0.1 as expected. The relative fluctuation of protonated disynaptic attractor V(C,H) of methyl group and both the rings is 0.34 and 0.31 respectively. The pyridine C–N and S=O bonds are delocalized with λ value of 0.52 and 0.64 respectively. The monosynaptic attractor V(N_{13}) has the highest λ value of 0.81 which indicates that the electrons get delocalized around the sulfonamide group.

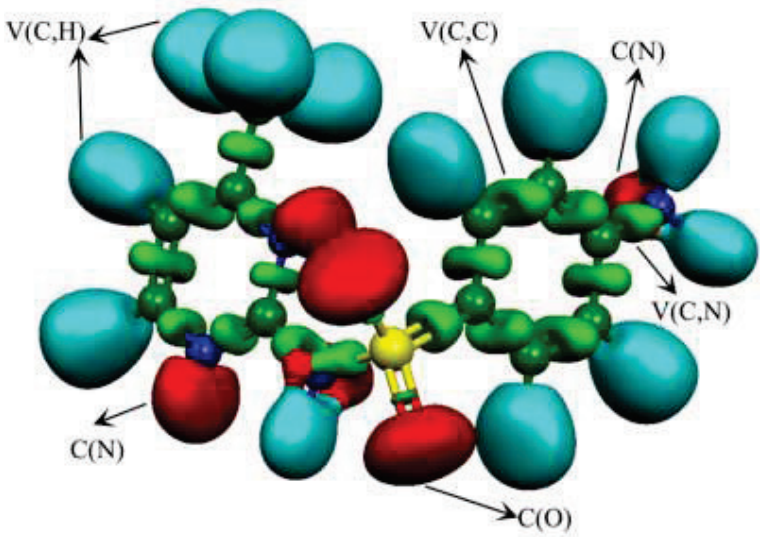

Fig. 6.2 Electron localization function value defining the bonding isosurface η(r) = 0.80 for sulfamerazine.

Table 6.4 Different types of electronic basins, ELF value at attractor (ELF), basin population (N), standard deviation (σ^2) and relative fluctuation (λ) of sulfamerazine.

BASINS	ELF	N	σ^2	λ	Total
$C(C_i)$	1.000	2.09	0.26	0.12	11
$C(N_i)$	1.000	2.10	0.30	0.14	4
C(S)	1.000	10.07	0.51	0.05	1
$C(O_i)$	1.000	2.12	0.34	0.16	2
$V(C_7,H_i)$	1.000	1.97	0.66	0.34	3
$V(C_i,H_j)$	1.000	2.16	0.67	0.31	6
$V(N_i,H_j)$	1.000	1.97	0.78	0.40	3
$V(C_1,C_i)$	0.943	2.86	1.34	0.47	2
$V(C_6,C_7)$	0.964	2.05	1.03	0.50	1
$V(C_i,C_j)$	0.940	2.84	1.35	0.48	6
$V(C_i,N_j)$	0.916	2.42	1.25	0.52	4
$V(N_i)$	0.964	2.82	1.19	0.42	2
$V(C_4,N_{13})$	0.929	2.02	1.07	0.53	1
$V(N_{13},S)$	0.898	1.71	1.00	0.58	1
$V(N_{13})$	0.830	0.59	0.48	0.81	1
$V(S,C_{18})$	0.950	2.23	1.13	0.51	1
$V(S,O_i)$	0.817	1.84	1.18	0.64	2
$V(O_i)$	0.889	2.57	1.22	0.47	2
$V(O_j)$	0.891	2.78	1.27	0.46	2
$V(C_{21},N_{28})$	0.928	2.14	1.14	0.53	1
$V(N_{28})$	0.933	1.70	0.93	0.55	1

6.5 Vibrational analysis

Experimental, simulated IR, Raman (higher region) and Raman (lower region) spectra of sulfamerazine are shown in Fig. 6.3, Fig. 6.4 and Fig. 6.5 respectively. The title compound has 30 atoms and 84 modes of vibration. Internal valence coordinates [71] of sulfamerazine has been defined in Table 6.5. Force constants of the symmetry coordinates and the scale factors used are given in Table 6.6. Scale factors have been

refined with an RMS error of 6.52 cm^{-1} between the experimental and SQM force field frequencies of the title compound. The vibrational assignments including experimental and calculated wavenumbers along with PED contributions are tabulated in Table 6.7.

6.5.1 Pyrimidine ring vibrations

The C−H stretching vibration of two nitrogen-substituted aromatic molecules such as pyrimidine gives rise to band in the region 3100 – 3010 cm^{-1} [103]. The weak band at 3004 cm^{-1} in the Raman spectrum is assigned to C−H stretching mode of pyrimidine (Pym) ring in the title compound. The C−C and C−N stretching vibrations of pyrimidine ring are expected in the region 1600 – 1500 cm^{-1} [103]. The strong intense band at 1568 cm^{-1} in IR is assigned to C−N stretching mode. The coupled C−C and C−N stretching vibration is found at medium intense band at 1506 cm^{-1} in Raman spectrum. The C−H in-plane and out-of-plane bending vibrations of the pyrimidine ring is characterized by several medium to strong intense bands in the region 1300 – 1000 cm^{-1} and 1000 – 650 cm^{-1} respectively [134]. The weak band at 1207 cm^{-1} in Raman identified as C−H in-plane stretching mode.

Table 6.5 Definition of internal valence coordinates of sulfamerazine.

No.	Symbol	Type	Definition
		Stretching	
1–2	R_i	C-C (ring)	C_1-C_2, C_6-C_1
3–6	R_i	C-N (ring A)	C_2-N_3, N_3-C_4, C_4-N_5, N_5-C_6
7–8	r_i	C-H (ring)	C_1-H_{11}, C_2-H_{12}
9	r_i	C-C (methyl)	C_6-C_7
10–12	r_i	C-H (methyl)	C_7-H_8, C_7-H_9, C_7-H_{10}
13	P_i	N-H (sulfonamide)	N_{13}-H_{14}
14	ξ_i	C-N (sulfonamide)	C_4-N_{13}

No.	Symbol	Type	Definition
15	ξ_i	N-S (sulfonamide)	N_{13}-S_{15}
16–17	R_i	S-O (sulfonamide)	S_{15}-O_{16}, S_{15}-O_{17}
18	r_i	S-C (sulfonamide)	S_{13}-C_{18}
19–24	R_i	C-C (ring)	C_{18}-C_{19}, C_{19}-C_{20}, C_{20}-C_{21}, C_{21}-C_{22}, C_{22}-C_{23}, C_{23}-C_{18}
25–28	r_i	C-H (ring)	C_{19}-H_{27}, C_{20}-H_{26}, C_{22}-H_{25}, C_{23}-H_{24}
29	r_i	C-N (amine)	C_{21}-N_{28}
30–31	Q_i	N-H (amine)	N_{28}-H_{29}, N_{28}-H_{30}
Bending			
31	α_i	C-C-C (ring)	C_6-C_1-C_2
32–36	α_i	C-N-C (ring A)	C_1-C_2-N_3, C_2-N_3-C_4, N_3-C_4-N_5, C_4-N_5-C_6, N_5-C_6-C_1
37–40	β_i	H-C-C (ring)	H_{11}-C_1-C_6, H_{11}-C_1-C_2, H_{12}-C_2-N_3, H_{12}-C_2-C_1
41–42	α_i	C-C-C (methyl)	C_7-C_6-C_1, C_7-C_6-N_5
43-45	α_i	H-C-H (methyl)	H_8-C_7-H_9, H_9-C_7-H_{10}, H_8-C_7-H_{10}
46-48	β_i	C-C-H (methyl)	C_6-C_7-H_{10}, C_6-C_7-H_9, C_6-C_7-H_8
49-50	θ_i	N-C-N (sulfonamide)	N_{13}-C_4-N_3, N_{13}-C_4-N_5
51	β_i	C-N-H (sulfonamide)	C_4-N_{13}-H_{14}
52	β_i	H-N-S (sulfonamide)	H_{14}-N_{13}-S_{15}
53	α_i	C-N-S (sulfonamide)	C_4-N_{13}-S_{15}
54	α_i	O-S-O (sulfonamide)	O_{16}-S_{15}-O_{17}
55	γ_i	N-S-C	N_{13}-S_{15}-C_{18}
56–57	β_i	O-S-C	O_{16}-S_{15}-C_{18}, O_{17}-S_{15}-C_{18}
58–59	β_i	O-S-N	O_{16}-S_{15}-N_{13}, O_{17}-S_{15}-N_{13}
60–61	β_i	S-C-C (chain)	S_{15}-C_{18}-C_{19}, S_{15}-C_{18}-C_{23}
62–67	α_i	C-C-C (ring)	C_{23}-C_{18}-C_{19}, C_{18}-C_{19}-C_{20}, C_{19}-C_{20}-C_{21}, C_{20}-C_{21}-C_{22}, C_{21}-C_{22}-C_{23}, C_{22}-C_{23}-C_{18}
68–75	β_i	H-C-C (ring)	H_{27}-C_{19}-C_{18}, H_{27}-C_{19}-C_{20}, H_{26}-C_{20}-C_{19}, H_{26}-C_{20}-C_{21}, H_{25}-C_{22}-C_{21}, H_{25}-C_{22}-C_{23}, H_{24}-C_{23}-C_{18}, H_{24}-C_{23}-C_{22}
76–77	α_i	N-C-C (amine)	N_{28}-C_{21}-C_{20}, N_{28}-C_{21}-C_{22}
78	ϕ_i	H-N-H (amine)	H_{29}-N_{28}-H_{30}
79–80	β_i	C-N-H (amine)	C_{21}-N_{28}-H_{29}, C_{21}-N_{28}-H_{30}

No.	Symbol	Type	Definition
Out-of-plane bending (wagging)			
81–82	ω_i	C-H (ring)	H_{11}-C_1-C_2-C_6, H_{12}-C_2-C_1-N_3
83	ω_i	C-C (methyl)	C_7-C_6-C_1-N_5
84	ω_i	C-N (sulfonamide)	N_{13}-C_4-N_3-N_5
85	ω_i	N-H (sulfonamide)	C_4-N_{13}-H_{14}-S_{15}
86	ω_i	S-C (sulfonamide)	S_{15}-C_{18}-C_{19}-C_{23}
87–90	ω_i	C-H (ring)	H_{27}-C_{19}-C_{18}-C_{20}, H_{26}-C_{20}-C_{19}-C_{21}, H_{25}-C_{22}-C_{21}-C_{23}, H_{24}-C_{23}-C_{18}-C_{22}
91	ω_i	C-N (amine)	N_{28}-C_{21}-C_{20}-C_{22}
92	ω_i	N-H (amine)	C_{21}-N_{28}-H_{29}-H_{30}
Torsion			
93–98	τ_i	C-C (ring)	C_6-C_1-C_2-N_3, C_1-C_2-N_3-C_4, C_2-N_3-C_4-N_5, N_3-C_4-N_5-C_6, C_4-N_5-C_6-C_1, N_5-C_6-C_1-C_2
99–104	τ_i	C-C (methyl)	H_8-C_7-C_6-C_1, H_8-C_7-C_6-N_5, H_9-C_7-C_6-C_1, H_9-C_7-C_6-N_5, H_{10}-C_7-C_6-C_1, H_{10}-C_7-C_6-N_5
105–108	τ_i	C-N (chain)	N_3-C_4-N_{13}-H_{14}, N_3-C_4-N_{13}-S_{15}, N_5-C_4-N_{13}-H_{14}, N_5-C_4-N_{13}-S_{15}
109–114	τ_i	N-S (sulfonamide)	C_4-N_{13}-S_{15}-O_{16}, C_4-N_{13}-S_{15}-O_{17}, C_4-N_{13}-S_{15}-C_{18}, H_{14}-N_{13}-S_{15}-O_{16}, H_{14}-N_{13}-S_{15}-O_{17}, H_{14}-N_{13}-S_{15}-C_{18}
115–120	τ_i	S-C (sulfonamide)	N_{13}-S_{15}-C_{18}-C_{19}, N_{13}-S_{15}-C_{18}-C_{23}, O_{16}-S_{15}-C_{18}-C_{19}, O_{16}-S_{15}-C_{18}-C_{23}, O_{17}-S_{15}-C_{18}-C_{19}, O_{17}-S_{15}-C_{18}-C_{23}
121–126	τ_i	C-C (ring)	C_{23}-C_{18}-C_{19}-C_{20}, C_{19}-C_{20}-C_{21}-C_{22}, C_{21}-C_{22}-C_{23}-C_{18}, C_{18}-C_{19}-C_{20}-C_{21}, C_{20}-C_{21}-C_{22}-C_{23}, C_{22}-C_{23}-C_{18}-C_{19}
127–130	τ_i	N-H (amine)	C_{20}-C_{21}-N_{28}-H_{29}, C_{20}-C_{21}-N_{28}-H_{30}, C_{22}-C_{21}-N_{28}-H_{29}, C_{22}-C_{21}-N_{28}-H_{30}

6.5.2 Phenyl ring vibrations

The various normal modes of substituted benzene ring are assigned according to Wilson's numbering convention [99]. The modes 2, 20a and 20b are classified as the C−H stretching modes of para substituted phenyl rings. The strong intense band at 3072 cm^{-1} in the Raman spectrum is assigned to mode 2. The normal modes 8a, 8b, 19a, 19b and 14 are C−C stretching vibrations of p-disubstituted phenyl rings. The modes 8a and 8b appears at 1570 – 1628 cm^{-1} and 1552 – 1605 cm^{-1} respectively. The mode 8a is observed as strong intense band at 1597 cm^{-1} in IR and 1594 cm^{-1} in

Raman. The medium intense band at 1558 cm^{-1} in Raman is assigned to mode 8b. The 19a and 19b modes appear as strong intense band at 1493 cm^{-1} and 1409 cm^{-1} in IR. Strong band at 1301 cm^{-1} in IR is assigned to mode 14. In p-disubstituted phenyl rings the C−H in-plane bending modes are classified as 3, 9a, 18a and 18b. The mode 3 normally appears very weak for p-disubstituted phenyl rings. The ring mode 9a appears at 1155 cm^{-1} and 1152 cm^{-1} in both IR and Raman respectively.

Table 6.6 Definition of local symmetry coordinates (much like the natural internal coordinates) and the corresponding force constant (mdyne/A°) of sulfamerazine with scale factors used.

No.	Symbol	Definition	Scale factors	Force constants (mdyne/Å)
Stretching				
1–2	Pym[νCC]	R_1, R_2	0.800	5.480
3–6	Pym[νCN]	R_3, R_4, R_5, R_6	0.984	7.154
7–8	Pym[νCH]	R_7, r_8	0.916	5.000
9	Me[νCC]	R_9	0.723	3.396
10	CH_{3ss}	$(r_{10}+r_{11}+r_{12})/\sqrt{3}$	0.895	4.780
11	CH_{3ips}	$(2r_{10}-r_{11}-r_{12})/\sqrt{6}$	0.895	4.702
12	CH_{3ops}	$(r_{11}-r_{12})/\sqrt{2}$	0.895	4.640
13	νNH	P_{13}	0.887	6.347
14	NH_{ss}	$(\xi_{14}+\xi_{15})/\sqrt{2}$	1.585	8.554
15	NH_{ips}	$(\xi_{14}-\xi_{15})/\sqrt{2}$	0.821	3.607
16	SO_{2ss}	$(R_{16}+R_{17})/\sqrt{2}$	0.957	8.858
17	SO_{2ips}	$(R_{16}-R_{17})/\sqrt{2}$	0.954	8.970
18	νSC	R_{18}	0.778	2.552
19–24	Ph[νCC]	R_{19}, R_{20}, R_{21}, R_{22}, R_{23}, R_{24}	0.980	6.421
25–28	Ph[νCH]	r_{25}, r_{26}, r_{27}, r_{28}	0.916	5.046
29	νCN	r_{29}	1.098	7.311
30	NH_{2ss}	$(Q_{30}+ Q_{31})/\sqrt{2}$	0.825	6.041
31	NH_{2ips}	$(Q_{30}- Q_{31})/\sqrt{2}$	0.895	6.571
Bending				
32	Pym_{trid}	$(\alpha_{31}- \alpha_{32}+ \alpha_{33}- \alpha_{34}+ \alpha_{35}- \alpha_{36})/\sqrt{6}$	0.989	1.412
33	Pym_{asyd}	$(2\alpha_{31}-\alpha_{32}-\alpha_{33}+2\alpha_{34}-\alpha_{35}-$	0.860	1.378

No.	Symbol	Definition	Scale factors	Force constants (mdyne/Å)
		$\alpha_{36})/\sqrt{12}$		
34	Pym_{asydo}	$(\alpha_{32}-\alpha_{33}+\alpha_{35}-\alpha_{36})/2$	0.903	1.219
35	Pym[δCH]	$(\beta_{37}-\beta_{38})/\sqrt{2}$	0.956	0.482
36	Pym[δNCH]	$(\beta_{39}-\beta_{40})/\sqrt{2}$	1.001	0.592
37	Me[δCC]	$(\alpha_{41}-\alpha_{42})/\sqrt{2}$	1.124	1.030
38	CH_{3sd}	$(\alpha_{43}+\alpha_{44}+\alpha_{45}-\beta_{46}-\beta_{47}-\beta_{48})/\sqrt{6}$	0.920	0.532
39	CH_{3ipb}	$(2\alpha_{43}-\alpha_{44}-\alpha_{45})/\sqrt{6}$	0.920	0.518
40	CH_{3opb}	$(\alpha_{44}-\alpha_{45})/\sqrt{2}$	0.920	0.517
41	CH_{3ipr}	$(2\beta_{46}-\beta_{47}-\beta_{48})/\sqrt{6}$	0.874	0.593
42	CH_{3opr}	$(\beta_{47}-\beta_{48})/\sqrt{2}$	0.874	0.553
43	Pym[δCN]	$(\theta_{49}-\theta_{50})/\sqrt{2}$	0.868	1.038
44	NH_{roc}	$(\beta_{51}-\beta_{52})/\sqrt{2}$	0.898	0.467
45	δCNS	$(2\alpha_{53}-\beta_{51}-\beta_{52})/\sqrt{6}$	0.866	0.467
46	SO_{2sci}	$(5\alpha_{54}+\gamma_{55})/\sqrt{26}$	0.795	1.460
47	SNC_{sci}	$(\alpha_{54}+5\gamma_{55})/\sqrt{26}$	0.860	1.396
48	SO_{2roc}	$(\beta_{56}-\beta_{57}+\beta_{58}-\beta_{59})/2$	0.948	1.394
49	SO_{2wag}	$(\beta_{56}+\beta_{57}-\beta_{58}-\beta_{59})/2$	0.892	1.671
50	SO_{2twi}	$(\beta_{56}-\beta_{57}-\beta_{58}+\beta_{59})/2$	0.898	0.934
51	δSC	$(\beta_{60}-\beta_{61})/\sqrt{2}$	0.866	0.757
52	Ph_{trid}	$(\alpha_{62}-\alpha_{63}+\alpha_{64}-\alpha_{65}+\alpha_{66}-\alpha_{67})/\sqrt{6}$	0.880	1.139
53	Ph_{asyd}	$(2\alpha_{62}-\alpha_{63}-\alpha_{64}+2\alpha_{65}-\alpha_{66}-\alpha_{67})/\sqrt{12}$	0.903	1.251
54	Ph_{asydo}	$(\alpha_{63}-\alpha_{64}+\alpha_{66}-\alpha_{67})/2$	0.880	1.100
55–58	Ph[δCH]	$(\beta_{68}-\beta_{69})/\sqrt{2}$, $(\beta_{70}-\beta_{71})/\sqrt{2}$, $(\beta_{72}-\beta_{73})/\sqrt{2}$, $(\beta_{74}-\beta_{75})/\sqrt{2}$	0.898	1.100
59	δCN	$(\beta_{76}-\beta_{77})/\sqrt{2}$	0.859	0.848
60	NH_{2sci}	$(2\phi_{78}-\beta_{79}-\beta_{80})/\sqrt{6}$	0.934	0.530
61	NH_{2roc}	$(\beta_{79}-\beta_{80})/\sqrt{2}$	0.491	0.322
Out-of-plane bending (wagging)				
62	Pym[gCH]	ω_{81}	0.830	0.363
63	Pym[gNCH]	ω_{82}	0.956	0.478
64	Me[gCC]	ω_{83}	1.047	0.640
65	Pym[gCN]	ω_{84}	0.920	0.628
66	gNH	ω_{85}	0.919	0.076
67	gSC	ω_{86}	0.830	0.335

No.	Symbol	Definition	Scale factors	Force constants (mdyne/Å)
68–71	Ph[gCH]	ω_{87}, ω_{88}, ω_{89}, ω_{90}	0.830	0.339
72	gCN	ω_{91}	0.920	0.657
73	gNH_2	ω_{92}	0.919	0.082
Torsion				
74	Pym_{puck}	$(\tau_{93}-\tau_{94}+\tau_{95}-\tau_{96}+\tau_{97}-\tau_{98})/\sqrt{6}$	1.639	0.490
75	Pym_{asyt}	$(\tau_{93}-\tau_{95}+\tau_{96}-\tau_{98})/2$	0.622	0.124
76	Pym_{asyto}	$(-\tau_{93}+2\tau_{94}-\tau_{95}-\tau_{96}+2\tau_{97}-\tau_{98})/\sqrt{12}$	0.622	0.144
77	τCH_3	$(\tau_{99}+\tau_{100}+\tau_{101}+\tau_{102}+\tau_{103}+\tau_{104})/\sqrt{6}$	1.051	0.003
78	τNH	$(\tau_{105}+\tau_{106}+\tau_{107}+\tau_{108})/2$	0.637	0.043
79	τNS	$(\tau_{109}+\tau_{110}+\tau_{111}+\tau_{112}+\tau_{113}+\tau_{114})/\sqrt{6}$	0.637	0.029
80	τSC	$(\tau_{115}+\tau_{116}+\tau_{117}+\tau_{118}+\tau_{119}+\tau_{120})/\sqrt{6}$	0.920	0.010
81	Ph_{puck}	$(\tau_{121}-\tau_{122}+\tau_{123}-\tau_{124}+\tau_{125}-\tau_{126})/\sqrt{6}$	1.030	0.378
82	Ph_{asyt}	$(\tau_{121}-\tau_{123}+\tau_{124}-\tau_{126})/2$	1.639	0.464
83	Ph_{asyto}	$(-\tau_{121}+2\tau_{122}-\tau_{123}-\tau_{124}+2\tau_{125}-\tau_{126})/\sqrt{12}$	1.030	0.359
84	τNH_2	$(\tau_{127}+\tau_{128}+\tau_{129}+\tau_{130})/2$	0.920	0.027

6.5.3 Sulfonamide group vibrations

The sulfamerazine molecule contains the secondary sulfonamide (SO_2NH) group. The N−H stretching vibration of sulfonamide is observed as a strong intense band at 3383 cm^{-1} in the IR spectrum. This band appears broad, as N−H of SO_2NH group of one molecule and nitrogen of pyrimidine ring of another molecule is involved in N−H···N hydrogen bonding. The symmetric and asymmetric stretching vibrations of SO_2 usually occur in the region 1180 – 1140 cm^{-1} and 1360 – 1315 cm^{-1} repectively [103]. The strong bands observed at 1090 cm^{-1} and 1095 cm^{-1} in the IR and Raman is assigned to SO_2 symmetric stretching vibrations. The symmetric stretching wavenumber is downshifted to 50 cm^{-1} from the given range due to the involvement of SO_2 group in N−H···O hydrogen bonding. The medium intense bands at 1301 cm^{-1} in IR and 1298 cm^{-1} in Raman is assigned to asymmetric SO_2 stretching

vibrations. The medium intense bands at 503 cm^{-1} in IR and 505 cm^{-1} in Raman is assigned to SO_2 scissoring vibration which usually appears in the region 586 – 504 cm^{-1}. SO_2 wagging vibration occurs in the region 551 – 438 cm^{-1} [30] which is obtained theoretically at 524 cm^{-1}. The medium intense band at 281 cm^{-1} in the Raman spectrum is assigned to SO_2 twisting vibration.

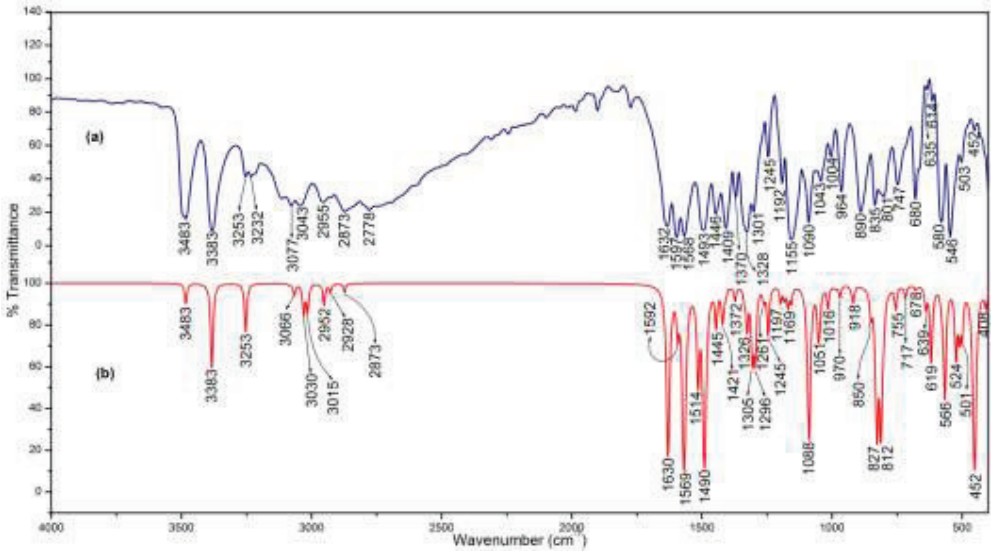

Fig. 6.3 (a) Experimental and (b) simulated IR spectra of sulfamerazine.

Table 6.7 Vibrational assignment of sulfamerazine by normal coordinate analysis based on SQM force field calculations.

Experimental (cm^{-1})		Calculated {B3LYP/6-311G(d, p)}			
υ_{IR}	υ_{Raman}	υ_{Scaled} (cm^{-1})	IR intensity (%)	Raman intensity (%)	Assignment (% PED, internal coordinates having contribution ≥10% are shown)
3483	-	3483	4.53	0.22	NH_{2ips}(100)
3383	-	3383	22.80	0.30	νNH(100)
3253	-	3253	11.64	0.94	NH_{2ss}(100)
3078	-	3084	0.30	0.21	Ph[νCH(99)]
-	3072	3067	0.47	0.33	Ph[νCH(99)]

Experimental (cm^{-1})		Calculated {B3LYP/6-311G(d, p)}			
υ_{IR}	υ_{Raman}	υ_{Scaled} (cm^{-1})	IR intensity (%)	Raman intensity (%)	Assignment (% PED, internal coordinates having contribution ≥10% are shown)
-	-	3066	2.12	0.67	Pym[νCH(99)]
3043	-	3031	3.81	0.50	Ph[νCH(99)]
-	-	3029	3.20	0.36	Ph[νCH(99)]
-	3004	3015	5.93	0.74	Pym[νCH(99)]
2955	-	2952	4.83	0.29	CH_{3ips}(98)
-	2925	2928	1.93	0.28	CH_{3ops}(100)
2873	-	2873	1.99	0.74	CH_{3ss}(98)
1632	1629	1630	77.69	1.12	NH_{2sci}(50) + Ph[νCC(21)] + νCN(19)
1597	1594	1593	9.35	0.55	Ph[νCC(49)] + NH_{2sci}(30) + Ph[δCH(13)]
1568	-	1569	100.00	0.96	Pym[νCN(55)] + Pym[δNCH(13)] + Pym_{asyd}(10)
-	1558	1559	0.93	0.05	Ph[νCC(74)]
-	1506	1514	26.55	0.03	Pym[νCN(50)] + Pym[νCC(20)]
1493	-	1492	13.74	0.25	Ph[νCC(35)] + Ph[δCH(32)] + νCN(16)
-	-	1490	81.89	0.15	NH_{ss}(25) + Pym[νCN(18)] + Pym[δNCH(12)] + NH_{ips}(11) + Ph_{trid}(10)
-	1446	1445	8.99	0.04	Pym[δCH(32)] + Pym[νCN(32)] + Pym[δNCH(12)]
-	1432	1421	7.64	0.16	CH_{3ipb}(79)
-	1413	1415	1.89	0.23	CH_{3opb}(91)
1409	-	1407	0.92	0.01	Ph[νCC(61)] + Ph[δCH(31)]
1370	1373	1372	3.13	0.13	Pym[δNCH(40)] + NH_{roc}(25) + Pym[νCN(15)]
1328	1332	1336	2.21	0.18	CH_{3sd}(93)
-	-	1326	9.95	0.13	νCN(40) + Ph[δCH(33)] + Ph[νCC(16)]

Experimental (cm^{-1})		Calculated {B3LYP/6-311G(d, p)}			
υ_{IR}	υ_{Raman}	υ_{Scaled} (cm^{-1})	IR intensity (%)	Raman intensity (%)	Assignment (% PED, internal coordinates having contribution ≥10% are shown)
1301	-	1306	18.15	0.13	Ph[νCC(69)] + SO_{2ips}(17)
-	1298	1295	19.02	0.08	SO_{2ips}(44) + Ph[νCC(41)]
-	-	1262	3.03	0.04	Ph[δCH(82)]
1245	-	1245	11.93	0.21	NH_{roc}(43) + SO_{2ips}(18)
-	1207	1197	3.64	0.05	Pym[νCN(65)] + Pym[δCH(20)] + Pym[νCC(12)]
1192	1191	1183	2.71	0.17	Pym[νCN(25)] + Pym[νCC(22)] + νCC(14) + Pym[δNCH(10)]
-	-	1169	4.57	0.01	Pym_{puck}(63) + gCC(10)
1155	1152	1157	3.55	0.08	Ph[δCH(83)] + Ph[νCC(13)]
-	-	1096	2.96	0.04	Ph[δCH(74)] + Ph[νCC(21)]
1090	1095	1088	59.97	1.88	SO_{2ss}(67) + Ph[νCC(10)]
1063	-	1053	9.18	0.56	Pym[νCC(27)] + Ph[νCC(26)] + Pym[νCN(11)] + Pym[δCH(10)]
1043	-	1048	7.21	0.27	Pym[νCC(29)] + Ph[νCC(18)] + Pym[νCN(11)] + SO_{2ss}(11)
1004	-	1016	5.01	0.10	Pym_{trid}(26) + CH_{3ipr}(20) + νCC(18)
-	999	988	0.49	0.02	Pym[gNCH(43)] + CH_{3opr}(40)
-	-	983	0.20	1.43	Pym[νCN(35)] + Pym_{trid}(31) + Pym[νCC(23)]
964	962	970	2.80	0.56	Ph_{trid}(58) + Ph[νCC(29)]
-	918	928	0.75	0.03	Pym[gNCH(44)] + CH_{3opr}(21) + Pym[gCN(14)]
890	894	918	3.80	0.03	CH_{3ipr}(44) + Pym[νCN(20)] + Pym[νCC(11)]
-	-	860	0.04	0.01	Ph[gCH(91)]
-	840	851	5.65	0.04	Ph[gCH(86)]

Experimental (cm^{-1})		Calculated {B3LYP/6-311G(d, p)}			
υ_{IR}	υ_{Raman}	υ_{Scaled} (cm^{-1})	IR intensity (%)	Raman intensity (%)	Assignment (% PED, internal coordinates having contribution ≥10% are shown)
835	-	827	59.09	0.03	NH_{ips}(23) + Ph[νCC(19)] + Ph_{trid}(10)
-	-	820	0.15	0.12	NH_{2roc}(84) + Ph[νCC(11)]
-	821	812	57.22	2.38	NH_{ips}(38) + NH_{ss}(12) + Ph_{trid}(10) + Ph[νCC(10)]
801	-	802	3.57	0.15	Ph[gCH(41)] + Ph_{asyt}(24) + Ph[gCN(22)]
-	-	755	5.06	0.01	Pym[gCH(88)]
747	742	728	0.10	0.06	Ph[gCH(98)]
-	715	717	2.77	1.16	Pym_{asydo}(30) + νCC(27) + Pym[νCC(15)]
680	682	678	0.98	0.01	Ph_{puck}(64) + Ph[gCH(16)]
-	659	640	4.89	0.59	Pym_{asyd}(47) + δCNS(10)
635	634	619	20.33	0.45	νSC(31) + Ph_{asyd}(28) + SO_{2wag}(12)
614	-	609	0.26	0.43	Ph_{asydo}(81)
580	586	578	2.67	0.06	gCNN(39) + gCC(26) + Pym_{asyt}(11)
546	549	566	34.97	0.15	Ph[gCH(35)] + Ph_{asyt}(23) + gSC(11)
-	-	524	18.15	0.51	SO_{2wag}(20) + Pym_{asydo}(14)
-	-	511	10.61	0.31	Pym_{asydo}(26) + SO_{2wag}(21) + νCC(14) + Ph_{asyd}(10)
503	505	500	11.36	0.07	SO_{2sci}(32) + Pym_{asyd}(10)
452	457	452	99.38	1.17	gNH_2(73) + νCN(14)
-	414	417	0.78	0.22	SO_{2roc}(18) + Ph_{asyto}(15) + gCC(10)
-	-	412	0.11	0.62	Ph_{asyto}(72) + Ph[gCH(18)]
-	-	408	4.21	0.46	gNH(22) + τNH(14) + τNS(14)
-	381	393	0.37	0.31	δCC(35)
-	-	360	3.14	0.44	Pym_{asyto}(22) + gCC(16) + gCNN(13)
-	-	340	0.12	0.34	δCN(45) + τNH_2(17) + SO_{2roc}(11)

Experimental (cm^{-1})		Calculated {B3LYP/6-311G(d, p)}			
υ_{IR}	υ_{Raman}	υ_{Scaled} (cm^{-1})	IR intensity (%)	Raman intensity (%)	Assignment (% PED, internal coordinates having contribution ≥10% are shown)
-	327	327	3.63	0.13	$\tau NH_2(73)$
-	-	315	0.68	0.57	$SO_{2sci}(20) + SNC_{sci}(12)$
-	300	298	3.77	0.44	$SO_{2sci}(12)$
-	281	271	0.43	0.60	$SO_{2twi}(45) + \nu SC(13)$
-	256	258	0.49	0.96	$\nu SC(25) + SO_{2twi}(13) + Ph_{asyd}(11)$
-	204	201	0.16	0.29	$Pym_{asyto}(31) + SNC_{sci}(14)$
-	-	177	1.68	0.27	$SNC_{sci}(30) + Pym_{asyto}(11)$
-	-	153	0.17	0.44	$\delta SC(59) + SO_{2roc}(18)$
-	113	125	0.30	1.85	$Pym_{asyt}(51) + Pym[gCH(24)]$
-	-	91	0.14	0.24	$\tau CH_3(64)$
-	84	88	0.51	4.89	$\delta CNS(23) + Pym_{asyt}(16) + gSC(15) + \tau NH(10) + \delta CNN(10)$
-	-	68	0.02	8.23	$gSC(30) + \tau NH(13) + Pym_{asyt}(11)$
-	-	40	0.32	55.4	$\tau SC(44) + \tau NS(21)$
-	-	24	0.06	75.5	$\tau NH(35) + gNH(32) + \tau SC(15)$
-	-	3	0.18	100.00	$\tau NS(40) + \tau NH(35) + \tau SC(10)$

Pym, Pyrimidine ring; Ph, phenyl ring; ν, stretching; δ, bending; τ, torsion; g, gauche; ss, symmetric stretching; ips, in plane stretching; ops, out of plane stretching; ipb, in plane bending; opb, out of plane bending; ipr, in plane rocking; opr, out of plane rocking; puck, puckering; trid, trigonal deformation; sd, symmetric deformation; asyd, asymmetric deformation; asydo, out of plane asymmetric deformation; asyt, asymmetric torsion; asyto, out of plane asymmetric torsion; sci, scissoring; roc, rocking; twi, twisting; wag, wagging.

6.5.4 Methyl group vibrations

Asymmetric and symmetric stretching modes of methyl group are expected in the region 2972 – 2952 cm^{-1} and 2882 – 2862 cm^{-1} [30] respectively. The in-plane stretching vibration of methyl group is observed at 2955 cm^{-1} in IR. The medium intense band observed at 2925 cm^{-1} in IR is assigned to out of plane stretching vibration of methyl. Strong intense band at 2873 cm^{-1} in FT-IR spectrum is assigned to symmetric stretching vibration. Medium intense band at 1413 cm^{-1} in FT-Raman and strong band at 1328 cm^{-1} in IR spectrum is assigned to methyl asymmetric and symmetric bending vibrations respectively. The less intense band at 1413 cm^{-1} in Raman spectrum and strong band at 1328 cm^{-1} in IR is assigned to methyl asymmetric and symmetric deformation vibrations.

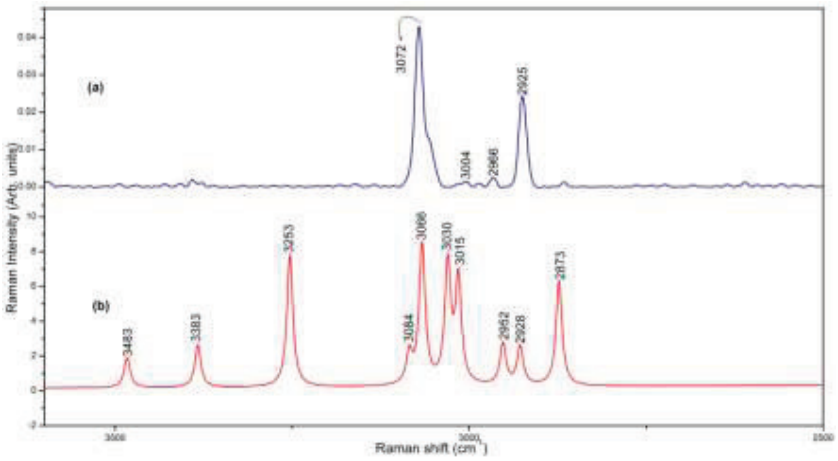

Fig. 6.4 (a) Experimental and (b) simulated Raman spectra of sulfamerazine (3600-2500 cm^{-1} region).

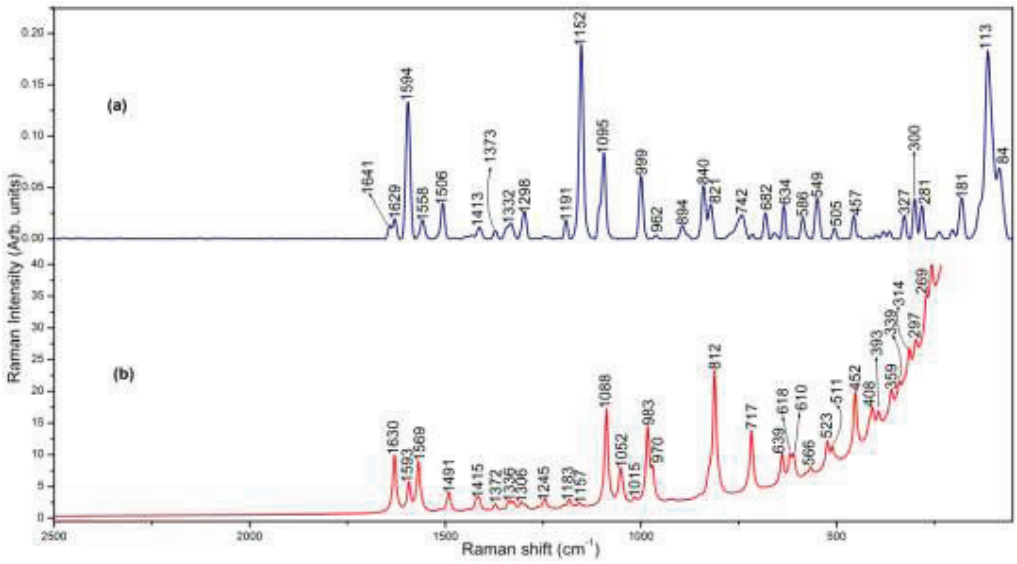

Fig. 6.5 (a) Experimental and (b) simulated Raman spectra of sulfamerazine (2500-50 cm^{-1} region).

6.5.5 Amine group vibrations

The asymmetric and symmetric stretching vibrations of primary amine are expected in the region 3500 – 3420 cm^{-1} and 3420 – 3340 cm^{-1} [101]. The broad intense band at 3483 cm^{-1} in IR is due to the in-plane stretching vibration of NH_2 group. The broad medium intense bands at 3253 cm^{-1} and 3232 cm^{-1} in IR is due to symmetric stretching vibration of NH_2 group. The NH_2 symmetric stretching is downshifted from the expected region due to the involvement of N−H in the N−H···O hydrogen bonding. The strong intense band at 1632 cm^{-1} in IR is assigned to NH_2 scissoring mode which is usually expected in the region 1650 – 1580 cm^{-1} [101]. The C−N stretching vibration is obtained at 1326 cm^{-1}. Normal coordinate analysis results predict that mode at 820 cm^{-1} is assigned to NH_2 rocking vibration.

6.6 Harmonic oscillator model of aromaticity (HOMA)

The aromaticity of sulfamerazine has been calculated from the molecular geometries obtained by using B3LYP/6-311G(d,p) method. The aromaticity values of

pyrimidine and phenyl rings of sulfamerazine based on harmonic oscillator model of aromaticity is found to be 0.9955 and 0.9622 respectively. The aromaticity of pyrimidine ring is significantly increased due to the attachment of electron donating methyl group to the ring system. The aromatic factor of phenyl ring got reduced due to the electron withdrawing SO_2NH group when compared to benzene (HOMA=1).

6.7 Conclusion

The molecular geometry of sulfamerazine is calculated using B3LYP/6-311G(d, p) basis set. Optimized geometrical parameters of the title compound are in good agreement with the reported structure, except some deviation due to intermolecular interaction in the crystalline state. The vibrational wavenumbers were calculated and assignments of vibrational modes have been performed. The charge transfer interaction between the methyl group and pyrimidine ring and the delocalization has been explained by natural bond orbital analysis. The delocalized bonds in the molecule are identified by electron localization function analysis. The delocalization of electrons around the electronegative nitrogen increases the stability of the antibacterial drug sulfamerazine. The molecule is further stabilized by strong intermolecular N−H···O and N−H···N interactions in the crystalline state. The aromaticity values of both the rings have been found based on harmonic oscillator model of aromaticity.